Mechanics of Advanced Materials and Structures

ISSN: 1537-6494 (Print) 1537-6532 (Online) Journal homepage: http://www.tandfonline.com/loi/umcm20

A Microstructure-Based Continuum Model for Multiphase Solids

Franck J. Vernerey

To cite this article: Franck J. Vernerey (2014) A Microstructure-Based Continuum Model for Multiphase Solids, Mechanics of Advanced Materials and Structures, 21:6, 441-456, DOI: 10.1080/15376494.2011.584149

To link to this article: https://doi.org/10.1080/15376494.2011.584149

Accepted author version posted online: 01 Nov 2013.
Published online: 01 Nov 2013.

Mechanics of Advanced Materials and Structures (2014) **21**, 441–456

ISSN: 1537-6494 print / 1537-6532 online
DOI: 10.1080/15376494.2011.584149

Taylor & Francis
Taylor & Francis Group

A Microstructure-Based Continuum Model for Multiphase Solids

FRANCK J. VERNEREY

Department of Civil, Environmental and Architectural Engineering, University of Colorado, Boulder, Colorado, USA

Received 27 August 2010; accepted 4 March 2011.

For applications in material design, it is critical that future material's models transition from empirically- to mechanistically-based. In this perspective, a continuum theory is introduced, based on a physically motivated strain decomposition, which not only reflects the macroscopic response of a solid but also the internal deformation and size effects of its microstructure. Because of the physical meaning of kinematic variables, constitutive relations may be derived from simple micromechanical arguments. Two examples are then presented: (a) the elastic response of an elastic material with defects and (b) the assessment of size effects at the boundary of a fiber-reinforced composite.

Keywords: composites, multiphasic models, defects, linear elasticity, enhanced continuum models

1. Introduction

In a number of applications, the mechanical behavior of materials exhibits a so-called size effect that may be observed in several instances, such as in the sensitivity of a material's response to the size of the specimen, as in the context of nano/microscopic specimen (MEMS) or during the localization material's deformation into a region of finite size during damage softening. For the prediction of such behavior, conventional continuum mechanics based on homogenization theory [1] is not preferred as it is insensitive to length scale and is known to lead to unphysical solutions for problems involving material instability and subsequent strain localization.

Different strategies have been introduced in the literature to address these issues and improve the continuum theory. There are two main types of approaches. The first approach consists of introducing a length scale in the model by defining a non-local strain measure [2, 3]. In other words, the strain is averaged in a domain whose size is related to the microstructure's intrinsic length. A second strategy is based on introducing a new term in the internal energy, which is associated with a strain gradient. This new quantity is usually negligible during homogeneous deformation but becomes predominant when the wavelength of deformation moves closer to the material's intrinsic length scale. In this context, a strain gradient theory was developed to characterize size effects in metals at the micron scale [4–6]. Similar approaches, namely the micropolar [7] and micromorphic theories [8, 9], were also used to study shear banding [10, 11] in granular materials and generally in plastic materials. A more recent development is the extension of the micromorphic theory to capture the evolution of damage in hierarchical materials [12, 13]. A strength of the aforementioned models resides in that they provide a mathematical basis on which to study size effects and allow continuum models to remain well-posed after the onset of material instability occurring during softening [3, 13, 14]. Their weakness resides in that they mostly rely on empirical constitutive relations since classical homogenization techniques are not valid for microstructural volumes that are small compared to the microstructure's intrinsic length scale. Furthermore, the physical meaning of a strain gradient is always hard to grasp; this complicates the determination of the constitutive relation even more.

The present article introduces a new continuum formulation for describing the deformation of solids whose microstructure consists of a population of heterogeneities embedded in a matrix material. The novelty of the approach resides in the definition of kinematic variables that are directly related to the deformation and evolution of the underlying microstructure. This description permits to have a direct relationship between the average material's behavior and microscopic mechanisms occurring at small scales. The strengths of the proposed approach are summarized as follows:

- Besides capturing the homogeneous material's behavior, the model permits to describe the internal deformation of the microstructure.
- An intrinsic length scale is naturally incorporated into the model.

Address correspondence to Franck J. Vernerey, Department of Civil, Environmental and Architectural Engineering, University of Colorado, Campus Box 428, Boulder, CO 80309-0428, USA. E-mail: franck.vernerey@colorado.edu
Color versions of one or more of the figures in the article can be found online at www.tandfonline.com/umcm.

- Kinematic variables are directly connected to physical quantities, which allow a derivation of the constitutive relation through simple micromechanics models.

The organization of the article is as follows. First, the basis of the theory is laid out, kinematic quantities are introduced, and governing equations are derived with the help of variational principles. A general form of the constitutive relation is then introduced, remaining on the context of linear elasticity. The presented theory is then related to three well-known assumptions regarding the deformation of defects in elastic solids: the mixture model, the dilute, and the Mori-Tanaka assumptions. The theory is then evaluated for two simple one-dimensional elastic problems: the volumetric deformation of an elastic material containing a population of defects and the size effects displayed by a fiber-reinforced composite near a stressed edge. For these examples, the constitutive relation is derived with micromechanical arguments and solutions can be computed analytically. In the second example, comparison between the model and actual results of a two-dimensional finite element simulation of a fiber-reinforced composite is also provided. Finally, concluding remarks are drawn.

2. Kinematics

In this article, we consider a material for which the microstructure consists of two phases: a matrix (denoted as "phase 1") and a population of heterogeneities (denoted as "phase 2"). The heterogeneities can be inclusions, voids, or fibers, depending on the material. Figure 1 shows a schematic of a typical biphasic microstructure.

A continuum description of such material generally relies on the concept of a homogenized strain that represents the average deformation in a microstructural element, called "representative volume element" (or RVE). Thus, if we introduce $\mathbf{u}$ as the displacement field in the RVE and $\mathbf{x}$ as the position of a material point in the deformed configuration, the variation of averaged strain $\delta\boldsymbol{\varepsilon}$ in the RVE Ω, subject to a variation $\delta\mathbf{u}$ of displacement is written in terms of the following averaging operation:

$$\delta\boldsymbol{\varepsilon} = \frac{1}{V}\int_{\Omega}\left(\frac{\partial\delta\mathbf{u}}{\partial\mathbf{x}}\right)_{sym} dV = \frac{V^1}{V}\left(\frac{1}{V^1}\int_{\Omega^1}\left(\frac{\partial\delta\mathbf{u}}{\partial\mathbf{x}}\right)_{sym} dV\right) + \frac{V^2}{V}\left(\frac{1}{V^2}\int_{\Omega^2}\left(\frac{\partial\delta\mathbf{u}}{\partial\mathbf{x}}\right)_{sym} dV\right), \tag{1}$$

where V, V_1 and V_2 are the volumes of the entire RVE, phase 1 and phase 2, respectively, and the subscript "*sym*" denotes the symmetric part of the associated tensor. At this point, it is useful to introduce several quantities: the volume fraction ω of phase 2 and the variations $\delta\mathbf{e}$ and $\delta\phi$ of average strain in phase 1 and phase 2, respectively, defined as follows:

$$\omega = \frac{V^2}{V} = 1 - \frac{V^1}{V}, \quad \delta\mathbf{e} = \frac{1}{V^1}\int_{\Omega^1}\left(\frac{\partial\delta\mathbf{u}}{\partial\mathbf{x}}\right)_{sym} dV, \quad \delta\phi = \frac{1}{V^2}\int_{\Omega^2}\left(\frac{\partial\delta\mathbf{u}}{\partial\mathbf{x}}\right)_{sym} dV. \tag{2}$$

As a result, the average strain increment in the RVE can be written in a simpler manner:

$$\delta\boldsymbol{\varepsilon} = (1-\omega)\,\delta\mathbf{e} + \omega\delta\phi. \tag{3}$$

This equation shows that the variation of continuum strain $\boldsymbol{\varepsilon}$ can be decomposed in a component in each phase. This decomposition is the basis of the definition of the independent kinematic variables for the microstructure-based continuum theory. A possibility is to choose a macroscopic displacement measure $\mathbf{u}$ and the average strain ϕ in heterogeneities as independent kinematic variables. In the case where $\omega \neq 0$, the strain variations $\delta\boldsymbol{\varepsilon}and\delta\mathbf{e}$ may then be obtained as a function of $\delta\mathbf{u}$ and $\delta\phi$ as follows:

$$\delta\boldsymbol{\varepsilon} = \left(\frac{\partial\mathbf{u}}{\partial\mathbf{x}}\right)_{sym} \quad \text{and} \quad \delta\mathbf{e} = \frac{1}{(1-\omega)}\left[\left(\frac{\partial\delta\mathbf{u}}{\partial\mathbf{x}}\right)_{sym} - \omega\delta\phi\right]. \tag{4}$$

The idea behind this decomposition is to provide an enriched description of the material deformation and the underlying mechanisms governing its mechanical response. Furthermore, because more kinematic variables are used, the governing equations will be different from that of a conventional continuum. We address this point in the next section.

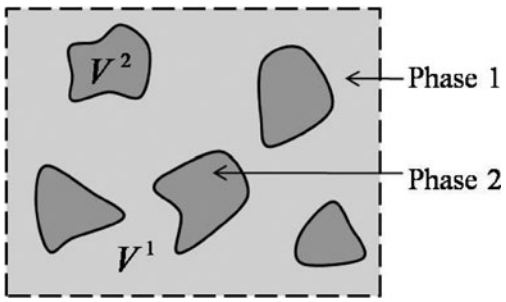

Fig. 1. Representative element of a biphasic material. Phase 1 is the matrix (of total volume V^1), while phase 2 represents heterogeneities in the form of voids, inclusions, or fibers (of total volume V^2).

3. Governing Equations

The mechanical response of a biphasic material depends on the relative properties of phases, as well as their topology and size. In particular, size effects observed during inhomogeneous deformation is usually attributed to the characteristic length-scale of the second phase (or heterogeneities). In order to account for these observations, we develop a microstructure-based theory based on the decomposition of the energy and governing equations of the two phases. Consider a two-phase

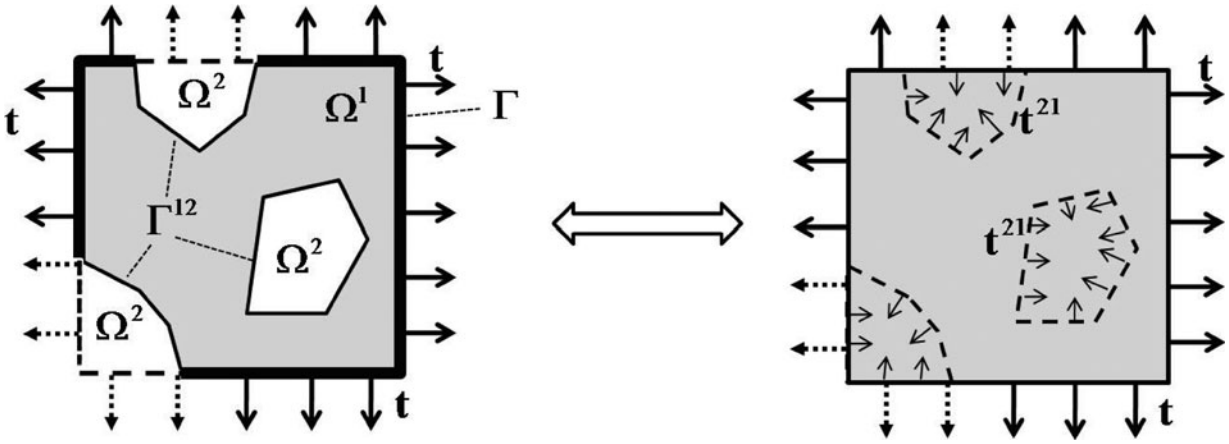

Fig. 2. Definition of interaction traction forces on phase 1. The traction forces are partitioned into those acting on phase 1 (solid arrows) and those acting on phase 2 (dashed arrows).

medium in a domain Ω delimited by a boundary Γ. We then consider the equilibrium of each phase independently and derive the governing equations.

3.1. *Equilibrium of Phase 1*

The condition for equilibrium of the first phase is written in terms of virtual energy principles as follows. Let us consider the material of phase 1 at equilibrium and apply a perturbation in the displacement field $\delta\mathbf{u}$ (denoted as virtual displacement). As a result of this virtual displacement, we can define a virtual internal energy δw^1_{int} (stored in phase 1) and a virtual external work of external forces acting on phase 1. In this analysis, we decompose the external work in two components: The virtual work δw^1_{ext} of forces that are external to the biphasic medium and the virtual work δw^{21} arising from forces exerted from phase 2 onto phase 1. For phase 1 to be at equilibrium, variational principles state that the virtual internal power is equal to the virtual work of external forces. We write:

$$0 = \delta w^1_{\text{int}} - \delta w^1_{ext} - \delta w^{21} \quad \text{where}$$
$$\times \begin{cases} \delta w^1_{\text{int}} = \displaystyle\int_\Omega (1-\omega)\,\boldsymbol{\sigma}^1 : \delta\mathbf{e}\,dV \\ \delta w^1_{ext} = \displaystyle\int_{\Omega^1} \rho^1\mathbf{b} : \delta\mathbf{u}\,dV + \int_\Gamma (1-\omega)\,\mathbf{t} : \delta\mathbf{u}\,dS \\ \delta w^{21} = \displaystyle\int_{\Gamma^{12}} \mathbf{t}^{21} : \delta\mathbf{u}\,dS \end{cases} . \quad (5)$$

The internal energy is conventional written in terms of the average stress $\boldsymbol{\sigma}^1$ and strain $\delta\mathbf{e}$ in phase 1, while the work of external forces (including δw^1_{ext} and δw^{21}) has three contributions:

- The external body forces $\mathbf{b}$.
- The traction forces $\mathbf{t}$ on the boundary Γacting on phase 1. For the sake of simplicity, we assume that the fractional area of phase 1 on any plane within the material is the same as the volume fraction $1-\omega$ of phase 1. This enables us to write the contribution of the surface traction in terms of ω and the surface integral over the total boundary Γ as seen in (5).
- The traction $\mathbf{t}^{21}$ arising from the interaction between phase 1 and 2. The traction vector $\mathbf{t}^{21}$ is interpreted as follows: Consider a small volume whose material properties are those of phase 1 and subject it to surface traction $\mathbf{t}$. The traction $\mathbf{t}^{21}$ is the traction to be applied on the boundary Γ^{12} for the deformation of phase 1 to be identical to that in the original biphasic medium (Figure 2).

Let us now examine the last term of (5). We assume that the traction $\mathbf{t}^{12}$ applied to the boundary between phase 1 and phase 2 can be written in terms of an interaction stress $\mathbf{h}^{21}$ as follows: $\mathbf{t}^{12} = \mathbf{h}^{12}\cdot\mathbf{n}$, where $\mathbf{n}$ is the unit normal vector to the boundary Γ^{12}. After a simple derivation (see the appendix), we show that the virtual work of traction forces $\mathbf{t}^{21}$ may be written in terms of the stress $\mathbf{h}^{12}$ and the average deformation of phase 2 as follows:

$$\delta w^{21} = \int_{\Gamma^{12}} \mathbf{t}^{21}\cdot\delta\mathbf{u}\,dS = \int_\Omega \omega\mathbf{h}^{21}\cdot\delta\phi\,dV. \quad (6)$$

The stress-like quantity $\mathbf{h}^{21}$ may then be interpreted as follows: it is the additional stress that must be added to the domain Ω_2, in a homogeneous medium with the properties of phase 1, such that the deformation of both phases is equivalent to that of the original biphasic medium. With this definition, one sees that if both phases have the same material properties, the stress $\mathbf{h}^{21}$ vanishes. Using (6), Eq. (5) can then be rewritten as:

$$\int_\Omega ((1-\omega)\boldsymbol{\sigma}^1 : \delta\mathbf{e} - (1-\omega)\rho^1\mathbf{b}\cdot\delta\mathbf{u} - \omega\mathbf{h}^{21} : \delta\phi)\,d\Omega$$
$$- \int_\Gamma ((1-\omega)\mathbf{t}\cdot\delta\mathbf{u})\,dS = 0. \quad (7)$$

Applying the divergence theorem and realizing that the above equation is valid for any RVE belonging to the body, we can write the governing equation such that equilibrium of phase 1

is satisfied:

$$\begin{cases} \nabla \cdot \boldsymbol{\sigma}^1 - (1-\omega)\,\rho^1 \mathbf{b} = 0 \\ -\boldsymbol{\sigma}^1 - \mathbf{h}^{21} = 0 \end{cases} \text{ in } \Omega \boldsymbol{\sigma}^1 \cdot \mathbf{n} = \mathbf{t} \text{ on } \Gamma. \quad (8)$$

3.2. *Equilibrium of Phase 2*

The equations for the equilibrium of phase 2 generally follow the same derivation as that of phase 1. The main difference resides in the fact that size effects associated with phase 2 are accounted for through the existence of strain gradient and stress couples in their internal energy. The stress couple may be interpreted as follows: when a variation of deformation occurs at the length-scale that is comparable to that associated to phase 2, there is an additional internal energy arising from the strain-gradient present in the inclusions. The couple stress is introduced to capture this additional energy, which ultimately results in introducing size effects into the model. This concept is, therefore, quite similar to those used in micromorphic and strain gradient theories. Thus, the equilibrium is written as follows:

$$0 = \delta w^2_{\text{int}} - \delta w^2_{ext} - \delta w^{12} \quad \text{where}$$
$$\times \begin{cases} \delta w^2_{\text{int}} = \int_\Omega \omega(\boldsymbol{\sigma}^2 : \delta\phi + \boldsymbol{\tau}^2 \vdots \delta\nabla\phi) dV \\ \delta w^2_{ext} = \int_{\Omega^2} (\rho^2 \mathbf{b} \cdot \delta\mathbf{u} + \mathbf{B} : \delta\phi) dV \\ \quad + \int_\Gamma \omega(\mathbf{t} \cdot \delta\mathbf{u} + \mathbf{T} : \delta\phi) dS \\ \delta w^{12} = \int_{\Gamma^{21}} \mathbf{t}^{12} : \delta\mathbf{u} dS \end{cases} . \quad (9)$$

The internal energy is written in terms of the stress $\boldsymbol{\sigma}^2$ and stress-couple $\boldsymbol{\tau}^2$ in phase 2, while the external work that arises can be decomposed into three contributions:

- The first contribution arises from external body forces $\mathbf{b}$ and external stress $\mathbf{B}$ on phase 2. The quantity $\mathbf{B}$ is associated with external physical processes leading to a deformation of phase 2. For instance, $\mathbf{B}$ may be the internal pressure in pore space.
- The second contribution comes from the presence of traction forces $\omega\mathbf{t}$ on the boundary Γ and the double traction $\omega\mathbf{T}$ arising from the external stress in phase 2 on the interface.
- Finally, the third contribution is a product of the traction $\mathbf{t}^{12}$ arising from the interaction between phase 2 and 1. The traction vector $\mathbf{t}^{12}$ is interpreted as follows: consider a small volume whose material properties are those of phase 2 and subject it to surface traction $\mathbf{t}$. The traction $\mathbf{t}^{12}$ is the traction to be applied on the boundary Γ^{12} for the deformation of phase 2 to be identical to that of the original biphasic medium (Figure 3).

Similar to our previous analysis, the interaction term is rewritten in terms of an interaction stress $\mathbf{h}^{12}$, representing the forces exerted by phase 1 on phase 2:

$$\delta w^{12} = \int_{\Gamma^2} \mathbf{t}^{12} : \delta\mathbf{u} dS = \int_\Omega (1-\omega)\mathbf{h}^{12} : \delta\mathbf{e} dV. \quad (10)$$

Using this expression, Eq. (9) can then be rewritten as follows:

$$\begin{aligned} &\int_\Omega \omega((\boldsymbol{\sigma}^2 - \mathbf{B}) : \delta\phi + \boldsymbol{\tau}^2 \vdots \delta\nabla\phi) d\Omega \\ &- \int_\Omega (\omega\rho^2 \mathbf{b} \cdot \delta\mathbf{u} + (1-\omega)\mathbf{h}^{12} : \delta\mathbf{e}) d\Omega \\ &- \int_\Gamma \omega(\mathbf{t} \cdot \delta\mathbf{u} + \mathbf{T} \cdot \delta\phi) dS = 0. \end{aligned} \quad (11)$$

Applying the divergence theorem and realizing that the above equation is valid for any RVE, we can write the governing equation, such that the equilibrium of phase 2 is satisfied:

$$\begin{cases} -\nabla \cdot \mathbf{h}^{12} - \omega\rho^2 \mathbf{b} = 0 \\ \boldsymbol{\sigma}^2 + \mathbf{h}^{12} - \nabla\boldsymbol{\tau}^2 - \mathbf{B} = 0 \end{cases} \text{ in } \Omega \quad \begin{cases} -\mathbf{h}^{12} \cdot \mathbf{n} = \mathbf{t} \\ \boldsymbol{\tau}^2 \cdot \mathbf{n} = \mathbf{T} \end{cases} \text{ on } \Gamma. \quad (12)$$

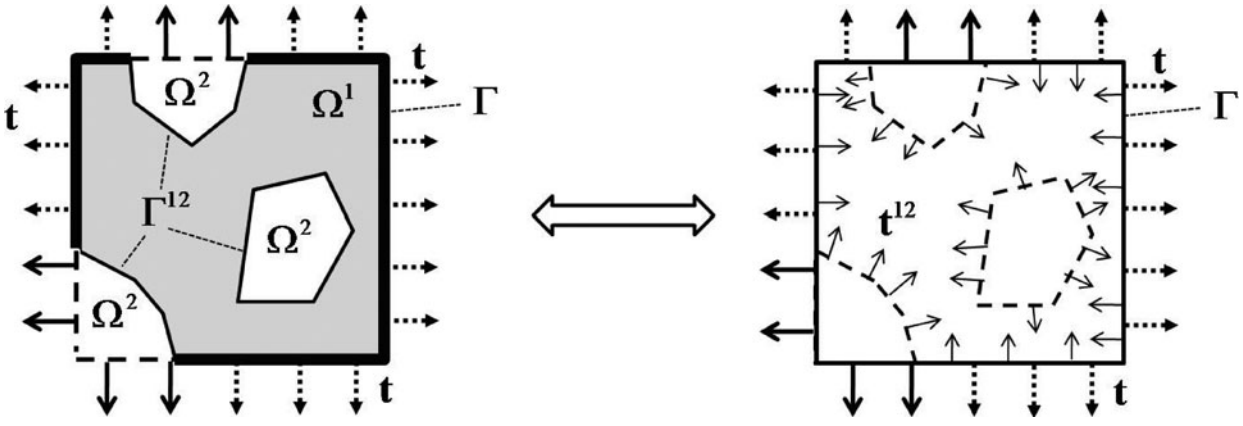

Fig. 3. Definition of interaction traction forces on phase 2. Here, the traction forces are partitioned into those acting on phase 2 (solid arrows) and those acting on phase 1 (dashed arrows).

3.3. *Equilibrium of the Biphasic Medium*

Similarly to mixture theory, the governing equations for the biphasic material are found by adding the governing equations for each phase. Thus, summing Eqs. (8) and (12), we find:

$$\begin{cases} \nabla \cdot (\boldsymbol{\sigma}^1 - \mathbf{h}^{12}) - \rho \mathbf{b} = 0 \\ (\boldsymbol{\sigma}^2 - \mathbf{h}^{21}) - (\boldsymbol{\sigma}^1 - \mathbf{h}^{12}) - \nabla \boldsymbol{\tau}^2 - \mathbf{B} = 0 \end{cases} \text{in } \Omega$$
$$\begin{cases} (\boldsymbol{\sigma}^1 - \mathbf{h}^{12}) \cdot \mathbf{n} = \mathbf{t} \\ \boldsymbol{\tau}^2 \cdot \mathbf{n} = \mathbf{T} \end{cases} \text{on } \Gamma, \tag{13}$$

where the density of the biphasic material $\rho = (1-\omega)\rho^1 + \omega\rho^2$ was used. In order to simplify the above equations, we introduce a new stress measure as follows:

$$\begin{cases} \mathbf{s}^1 = \boldsymbol{\sigma}^1 - \mathbf{h}^{12} \\ \mathbf{s}^2 = \boldsymbol{\sigma}^2 - \mathbf{h}^{21} \end{cases}, \tag{14}$$

which enables us to write (13) in the simpler form:

$$\begin{cases} \nabla \cdot \mathbf{s}^1 - \rho \mathbf{b} = 0 \\ \mathbf{s}^2 - \mathbf{s}^1 - \nabla \boldsymbol{\tau}^2 - \mathbf{B} = 0 \end{cases} \text{in } \Omega \begin{cases} \mathbf{s}^1 \cdot \mathbf{n} = \mathbf{t} \\ \boldsymbol{\tau}^2 \cdot \mathbf{n} = \mathbf{T} \end{cases} \text{on } \Gamma. \tag{15}$$

We obtain a system of two coupled differential equations for the equilibrium of forces in the matrix and the balance of forces between the matrix and heterogeneities. Let us ignore body forces for now and make several observations.

(i) In the case $\omega = 0$, the matrix strain equates the total strain ($\mathbf{e} = \boldsymbol{\varepsilon}$ from Eq. 3) and the above analysis leads to the following governing equations:

$$\nabla \cdot \boldsymbol{\sigma}^1 - \rho \mathbf{b} = 0 \quad \text{in } \Omega \qquad \boldsymbol{\sigma}^1 \cdot \mathbf{n} = \mathbf{t} \quad \text{on } \Gamma,$$

and $\mathbf{h}^{12} = 0$. In other words, one obtains the governing of a homogeneous Cauchy continuum, representing the matrix material without heterogeneities.

(ii) In the case $\omega = 1$, the heterogeneity strain equates the total strain ($\phi = \boldsymbol{\varepsilon}$ from Eq. 3) and we can show that the following governing equation is obtained

$$\nabla \cdot (\boldsymbol{\sigma}^2 - \mathbf{B}) - \nabla^2 \cdot \boldsymbol{\tau}^2 - \rho \mathbf{b} = 0 \quad \text{in } \Omega$$
$$\begin{cases} \mathbf{s}^2 \cdot \mathbf{n} = \mathbf{t} \\ \boldsymbol{\tau}^2 \cdot \mathbf{n} = \mathbf{T} \end{cases} \text{on } \Gamma,$$

and $\mathbf{h}^{21} = 0$. The above equation represents the equilibrium of a strain gradient sensitive material. Such size sensitive mechanical models have been introduced to explain the size dependency of material response at small scales and, in particular, size dependent plasticity [4, 5].

(iii) Now considering the case of an arbitrary volume fraction ω and assuming that the strains are macroscopically homogeneous (this means that the couple stress vanishes and thus $\nabla \cdot \boldsymbol{\tau}^2 = 0$), the second equation in (15) becomes $\mathbf{s}^2 = \mathbf{s}^1$. This is interpreted as the equilibrium between driving forces for matrix and heterogeneities deformations.

4. Elastic Constitutive Relation

4.1. *Deformation and Interaction Energies*

In this article, we limit our study to linear elastic material behavior in order to put an emphasis on the coupling between the internal forces acting on different phases. Our derivation is based on the decomposition of the density of stored elastic energy into a component w^1 associated with phase 1, a component w^2 associated with phase 2, and a component representing the interactions between the two phases. To characterize the behavior of each phase independently, we introduce a quadratic form for the internal energies w^1_{int}, w^2_{int} as follows:

$$\begin{cases} w^1_{\text{int}} = \dfrac{(1-\omega)}{2} \mathbf{e} : \mathbf{C}^1 : \mathbf{e} \\ w^2_{\text{int}} = \dfrac{\omega}{2} \left(\phi : \mathbf{C}^2 : \phi + \nabla\phi \dot{:} \mathbf{G}^2 \dot{:} \nabla\phi \right) \end{cases}, \tag{16}$$

where $\mathbf{C}^1$ and $\mathbf{C}^2$ are the elastic moduli of the phase 1 and 2, respectively. The third order tensor $\mathbf{G}^2$ is an elastic tensor that characterizes the resistance of the material to the gradient of the deformation of phase 2.

There are two interaction energies: the energy w^{21} associated with the work of the force exerted by phase 2 on phase 1, and the energy w^{12} associated with the work of phase 1 on phase 2. From the principle of action and reaction, these energies should be opposite to one another, that is: $w^{12} = -w^{21}$. A simple expression for these energies is given in terms of an "interaction matrix" $\mathbf{A}$ as follows:

$$w^{12} = -w^{21} = -\omega(1-\omega)\mathbf{e} : \mathbf{A} : \phi. \tag{17}$$

4.2. *Linear Elastic Relation*

From Eqs. (5), (6), (9), and (10), one can derive the relationship between stress measures and internal and interaction energies:

$$(1-\omega)\boldsymbol{\sigma}^1 = \frac{\partial w^1}{\partial \mathbf{e}}, \quad \omega\boldsymbol{\sigma}^2 = \frac{\partial w^2}{\partial \phi}, \quad (1-\omega)\mathbf{h}^{12} = \frac{\partial w^{12}}{\partial \mathbf{e}},$$
$$\omega\mathbf{h}^{21} = \frac{\partial w^{21}}{\partial \phi}, \quad \omega\boldsymbol{\tau}^2 = \frac{\partial w^2}{\partial \nabla\phi}. \tag{18}$$

A linear constitutive relation for $\mathbf{s}^1$, $\mathbf{s}^2$, and $\boldsymbol{\tau}^2$ can then be found using (16) and (17):

$$\begin{cases} \mathbf{s}^1 = \boldsymbol{\sigma}^1 - \mathbf{h}^{12} = \dfrac{1}{(1-\omega)} \left(\dfrac{\partial w^1}{\partial \mathbf{e}} - \dfrac{\partial w^{12}}{\partial \mathbf{e}} \right) \\ \quad = \mathbf{C}^M : \mathbf{e} + \omega \mathbf{A} : \phi \\ \mathbf{s}^2 = \boldsymbol{\sigma}^2 - \mathbf{h}^{21} = \dfrac{1}{\omega} \left(\dfrac{\partial w^2}{\partial \phi} - \dfrac{\partial w^{21}}{\partial \phi} \right) \\ \quad = \mathbf{C}^H : \phi - (1-\omega)\mathbf{A}^T : \mathbf{e} \\ \boldsymbol{\tau}^2 = \dfrac{1}{\omega} \dfrac{\partial w^2}{\partial \nabla\phi} = \mathbf{G} \dot{:} \nabla\phi \end{cases}. \tag{19}$$

Rewriting all stresses and strains in the Voight notation and assembling them into a vector, the constitutive relation can be

rewritten in a more familiar form as follows:

$$\begin{pmatrix} \mathbf{s}^1 \\ \mathbf{s}^2 \\ \boldsymbol{\tau}^2 \end{pmatrix} = \begin{bmatrix} \mathbf{C}^1 & \omega\mathbf{A} & 0 \\ -(1-\omega)\,\mathbf{A}^T & \mathbf{C}^2 & 0 \\ 0 & 0 & \mathbf{G} \end{bmatrix} \cdot \begin{pmatrix} \mathbf{e} \\ \phi \\ \nabla\phi \end{pmatrix}. \tag{20}$$

This formulation, therefore, clearly separates the contribution from matrix, heterogeneity, and their interactions; this facilitates the derivation of a constitutive relation.

4.3. *Overall Stress*

Upon solving the governing equations, the overall stress $\boldsymbol{\sigma}$ in the composite can be calculated by averaging the stress in the RVE. This is similar to the approach used to decompose the overall strain increment into a contribution from each phase in (1), (2), and (3). This gives:

$$\boldsymbol{\sigma} = (1-\omega)\,\boldsymbol{\sigma}^1 + \omega\boldsymbol{\sigma}^2. \tag{21}$$

In the remainder of the article, we propose to investigate the solution of simple linear elastic problems to illustrate the power of the microstructure-based theory.

5. Link with Known Micromechanical Models

We first consider the case of homogeneous deformation of a class of solids possessing a population of small elastic inclusions (or defects) embedded in an elastic matrix. Since homogeneous deformation is considered, the spatial gradient of inclusion deformation ϕ vanishes and the governing equations (15) and constitutive relations (20) simplify to:

$$\begin{cases} \nabla\cdot\mathbf{s}^1 = 0 \\ \mathbf{s}^1 - \mathbf{s}^2 = 0 \end{cases} \text{in}\Omega \quad \text{and} \quad \begin{pmatrix} \mathbf{s}^1 \\ \mathbf{s}^2 \end{pmatrix} = \begin{bmatrix} \mathbf{C}^M & \omega\mathbf{A} \\ -(1-\omega)\,\mathbf{A}^T & \mathbf{C}^H \end{bmatrix} \cdot \begin{pmatrix} \mathbf{e} \\ \phi \end{pmatrix}. \tag{22}$$

Thus, the problem is entirely defined if we know the elastic moduli of the matrix and defect, $\mathbf{C}^M$ and $\mathbf{C}^H$, respectively, and the interaction matrix $\mathbf{A}$. While the first two moduli are usually known, the interaction matrix depends on inclusion geometry, volume fraction, as well as the difference between material properties of the matrix and defects. In the case of small defect volume fraction, we can assume that no interaction exists between adjacent inclusions. In this case, we can write a linear relationship between the overall infinitesimal strain $\boldsymbol{\varepsilon}$ and the deformation ϕ of an inclusion in terms of the strain concentration tensor $\mathbf{M}$ as follows:

$$\phi = \mathbf{M} : \boldsymbol{\varepsilon}. \tag{23}$$

Using the above equation together with the constitutive relation and the second governing equation in (22) leads to an equation for the coefficients of the transfer matrix $\mathbf{A}$ as follows:

$$\omega\mathbf{A}\cdot\mathbf{M} + \mathbf{A}^T(\mathbf{I}-\omega\mathbf{M}) = \mathbf{C}^H\cdot\mathbf{M} - \frac{\mathbf{C}^M}{1-\omega}(\mathbf{I}-\omega\mathbf{M}). \tag{24}$$

Thus, the knowledge of the matrix $\mathbf{M}$ is enough to determine the interaction matrix $\mathbf{A}$ in this particular case. In the case of a linear elastic material, which possesses a distribution of elliptical defects at small volume fraction, a relationship between the average strain in the matrix and the strain in the defect may be determined from micromechanical arguments. We examine three common models: the mixture model, the dilute composite model, and the Mori-Tanaka model, [15, 16], each of them representing a different level of approximation.

5.1. *Mixture Model*

The mixture model represents the coarser level of approximation. In this model, the deformation of inclusions and matrix is assumed to be the same, regardless of their relative properties. This may be written as:

$$\boldsymbol{\phi} = \mathbf{e} = \boldsymbol{\varepsilon}. \tag{25}$$

It is, therefore, straightforward to derive the strain concentration tensor $\mathbf{M}$ appearing in (23):

$$\mathbf{M} = \mathbf{I}. \tag{26}$$

5.2. *Dilute Composite Model*

When the volume fraction of inclusions is sufficiently small, Mura [15, 16] introduced a method to derive the strain-concentration tensor in terms of the elastic properties of the matrix and inclusion as well as inclusion topology. The method basically consists of replacing the actual inclusion (with elastic modulus $\mathbf{C}^H$) by an equivalent "homogeneous" inclusion that has the same properties ($\mathbf{C}^M$) as the matrix and that is subject to an eigenstrain $\boldsymbol{\varepsilon}^*$. The eigenstrain is defined by the strain of the inclusion, in an unconstrained state. The eigenstrain is chosen such that the stress state in the inclusion is the same in actual composite and in the equivalent homogeneous medium. This reads as:

$$\mathbf{C}^H : \boldsymbol{\phi} = \mathbf{C}^M : (\boldsymbol{\phi} - \boldsymbol{\varepsilon}^*). \tag{27}$$

The next step consists of determining an expression of the eigenstrain, in terms of the deformation of the inclusion and the matrix. Using the definition of the Eshelby tensor $\mathbf{S}$, a relationship exists between $\boldsymbol{\phi}$, $\boldsymbol{\varepsilon}$, and $\boldsymbol{\varepsilon}^*$ as follows:

$$\boldsymbol{\phi} = \boldsymbol{\varepsilon} + \mathbf{S} : \boldsymbol{\varepsilon}^*. \tag{28}$$

The Eshelby tensor typically carries the information about the properties and aspect ratio of elliptical inclusions for which expressions can be found in [15, 16]. Using (27) and (28), it is straightforward to determine the relationship between

$\boldsymbol{\phi}$ and $\boldsymbol{\varepsilon}$, leading to the following expression for the strain concentration tensor:

$$\mathbf{M} = [\mathbf{I} + \mathbf{S} : \mathbf{C}^{-M} : (\mathbf{C}^{H} - \mathbf{C}^{M})]^{-1}, \tag{29}$$

where $\mathbf{C}^{-M}$ is the inverse of $\mathbf{C}^{M}$. It has to be noted that the assumptions used in (27) and (28) are valid when the inclusions are dilutely dispersed in the matrix and, therefore, do not feel the presence of their neighbors. This assumption for dilute composite is generally true when the volume fraction of ω inclusions is smaller than 0.1. Thus, for dilute composites, the interaction matrix $\mathbf{A}$ is found by substituting the expression for $\mathbf{M}$ in (24) and solving the system.

5.3. *Mori-Tanaka Model*

When the volume fraction of inclusions is greater than 0.1, the dilute approximation breaks down and it is necessary to account for the effect of interactions between neighboring inclusions. The Mori-Tanaka method provides a solution to this problem by assuming that the stress acting on heterogeneities arises from two contributions: the far field stress and an additional stress resulting from the interaction between inclusions. Referring to Benveniste [17], the strain in the inclusion $\boldsymbol{\phi}$ is related to the strain $\mathbf{e}$ in the matrix (that accounts for local variations) through a strain concentration tensor $\mathbf{M}^{h}$. Similarly, the strain in the matrix is related to the overall strain $\boldsymbol{\varepsilon}$ by a strain concentration tensor $\mathbf{M}^{m}$. This can be written as:

$$\begin{aligned} \mathbf{e} &= \mathbf{M}^{m} : \boldsymbol{\varepsilon} \\ \boldsymbol{\phi} &= \mathbf{M}^{h} : \mathbf{e} = \mathbf{M}^{h} : (\mathbf{M}^{m} : \boldsymbol{\varepsilon}) . \end{aligned} \tag{30}$$

Note that the dilute case is retrieved if the strain in the matrix is the same as the overall strain, that is $\mathbf{M}^{m} = \mathbf{I}$. Now, using the fact that $\boldsymbol{\varepsilon} = (1 - \omega)\,\mathbf{e} + \omega\phi$, we can derive a relationship between $\mathbf{M}^{m}$ and $\mathbf{M}^{h}$ as follows:

$$\mathbf{M}^{m} = [\omega\mathbf{M}^{h} + (1 - \omega)\mathbf{I}]^{-1}. \tag{31}$$

Various forms may be derived for the strain concentration $\mathbf{M}^{h}$. In particular, we can use the expression derived in the previous section, which leads to the Mori-Tanaka expressions for $\mathbf{M}^{h}$ and $\mathbf{M}^{m}$:

$$\begin{cases} \mathbf{M}^{h} = [\mathbf{I} + \mathbf{S} : \mathbf{C}^{-M} : (\mathbf{C}^{H} - \mathbf{C}^{M})]^{-1} \\ \mathbf{M}^{m} = [(1 - \omega)\mathbf{I} + \omega[\mathbf{I} + \mathbf{S}\mathbf{C}^{-M}(\mathbf{C}^{H} - \mathbf{C}^{M})]^{-1}]^{-1} \end{cases} . \tag{32}$$

Thus, the concentration tensor $\mathbf{M}$ used in (23) is simply:

$$\mathbf{M} = \mathbf{M}^{h} : \mathbf{M}^{m}. \tag{33}$$

This expression for $\mathbf{M}$ can then be used in (24), in order to determine the form of the interaction matrix $\mathbf{A}$ in the microstructure-based theory. It should be noted that the Mori-Tanaka model is valid for a volume fraction smaller than 0.25. In order to illustrate how the Mori-Tanaka model is incorporated into the microstructure-based theory, we propose to investigate a simple one-dimensional example of the volumetric deformation of an elastic material with defects.

6. Application 1: Volumetric Deformation of an Elastic Medium with Voids

We now consider the problem of an elastic solid under volumetric stress state as depicted by the left-hand side of Figure 4. In this case, the displacements are the same in the x and y direction. For simplicity, we only consider the displacement u in the x-direction, reducing the problem to a one-dimensional analysis. Furthermore, due to the symmetry of the problem, we only consider material points belonging to the segment $x \in [0, L]$ (right-hand side of the volume represented in Figure 4).

6.1. *Governing Equations*

In this problem, the overall deformation is homogeneous. This means the contribution from the stress couple $\boldsymbol{\tau}^{2}$ in the governing equations (15) vanishes and we obtain:

$$\begin{cases} \dfrac{\partial s^{1}}{\partial x} = 0 \\ s^{1} - s^{2} = 0 \end{cases} \qquad x \in [0, L] . \tag{34}$$

Assuming that there is no rigid body motion, the boundary conditions are zero displacement u in the center ($x = 0$) of

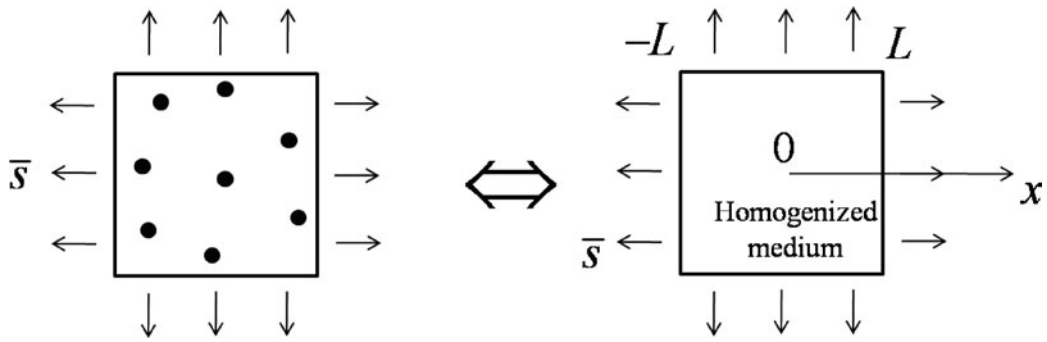

Fig. 4. Original problem and one-dimensional equivalent model.

the domain and an overall stress $\bar{s}$ on the external boundary ($x = L$) of the domain. This leads to:

$$\begin{cases} u(0) = 0 \\ \bar{\sigma} = (1-\omega)\, K^M e(L) + \omega K^I \phi(L) \end{cases} \Rightarrow \begin{cases} u(0) = 0 \\ e(L) = \bar{\sigma}/((1-\omega)K^M) \end{cases}, \tag{35}$$

where we used the fact that $\bar{\sigma}(L) = (1-\omega)\,\sigma^m + \omega\sigma^h$ and $K^I = 0$ (inclusions are voids).

6.2. *Constitutive Relation*

For this one-dimensional problem, the elasticity matrix has the form given in (22) by replacing the elastic moduli $\mathbf{C}^M$ and $\mathbf{C}^H$ by their bulk modulus K^M and K^H. Furthermore, since inclusions are replaced with voids, we have $K^H = 0$. Referring to Eq. (22), the elastic constitutive relation is written in terms of the elastic properties of the matrix K^M and the interaction matrix A:

$$\begin{pmatrix} s^1 \\ s^2 \end{pmatrix} = \begin{bmatrix} K^M & \omega A \\ -(1-\omega)\, A & 0 \end{bmatrix} \cdot \begin{pmatrix} e \\ \phi \end{pmatrix}. \tag{36}$$

The determination of the interaction matrix (here a scalar quantity) is straightforward by solving (24), now a scalar equation. The relationship between the strain concentration tensor M, the bulk modulus K^M, and A is then:

$$A = \frac{\omega M - 1}{1-\omega} K^M. \tag{37}$$

6.3. *Solution*

The governing equations together with the constitutive relation are now solved using the following simple procedure:

- First of all, the first equation in (34) implies that the stress s is constant.
- Using the fact that $\bar{\sigma} = (1-\omega)\, K^M e$, the matrix strain e is found to be constant and equal to $e(x) = \bar{\sigma}/(1-\omega)K^M$.
- The expression for e is then substituted in the constitutive relation (36), which permits to calculate the quantities s^1 and s^2 in terms of ϕ and $\bar{\sigma}$.
- Using the second equation in (34), we determine the void deformation ϕ in terms of the applied stress $\bar{\sigma}$.
- The overall stress and strain are then computed using $\begin{cases} \varepsilon = (1-\omega)\, e + \omega\phi \\ \sigma = (1-\omega)\, K^H e \end{cases}$.

We now solve the system of equations for three well-known models: the mixture model, the dilute composite model, and the Mori-Tanaka model. As defined in the previous section, each model is characterized by a different strain concentration tensor $\mathbf{M}$, and thus, a different interaction matrix $\mathbf{A}$. We then examine the interaction matrix and the overall behavior of the composite for each model.

6.3.1. *Mixture Theory*

For the mixture model, the strain intensity tensor $\mathbf{M}$ and the interaction matrix $\mathbf{A}$ are computed from (26) and (37):

$$M = 1 \Rightarrow A = -K^M. \tag{38}$$

Using this expression of A in (36) leads to the following relations:

$$\bar{\sigma} = (1-\omega)\, K^M \varepsilon \quad \text{and} \quad e = \phi = \varepsilon. \tag{39}$$

Consistent with the assumption of the mixture theory, we find that the strain is the same in the voids and in the matrix. For this particular example, this approximation is not appropriate since the deformation of voids is generally significantly higher than that of the matrix.

6.3.2. *Dilute Composite Model*

In the dilute composite model, referring again to (29) and (37), the strain intensity tensor M and the interaction matrix A take the form:

$$M = \frac{1}{1-S} \quad \Rightarrow \quad A = -K^M \frac{1-S-\omega}{(1-S)(1-\omega)}, \tag{40}$$

where the Eshelby tensor (now a scalar quantity) takes the value $S = 2/5(1-\nu)$ [16] for the geometry and loading considered and ν is the Poisson's ratio of the material. Again, using this expression of A in (36) leads to the following relations:

$$\bar{\sigma} = \left(K^M \frac{1-S-\omega}{1-S} \right) \varepsilon, \quad e = \frac{(1-S-\omega)\,\varepsilon}{(1-\omega)(1-S)} \quad \text{and} \quad \phi = \frac{\varepsilon}{1-S}. \tag{41}$$

In this case, we notice that the strain in the inclusion depends on the Eshelby tensor. This means that the shape and properties of the inclusion are taken into account. However, notice that ϕ is independent of the volume fraction ω, which is consistent with the assumption that the inclusion only feels the effect from the far-field stress, and thus does not depend on the surrounding inclusions.

6.3.3. *Mori-Tanaka Model*

For the Mori-Tanaka method, the strain intensity tensor M may then be determined with (37) for which the expressions of M^h, M^m follow from Eq. (32):

$$M^h = \frac{1}{1-S} \quad \text{and} \quad M^m = \frac{1-S}{(1-\omega)(1-S)+\omega}, \tag{42}$$

where once again, $S = 2/5(1-\nu)$ [16]. Referring to Eq. (37), this leads to:

$$M = M^h M^m = \frac{1}{(1-\omega)(1-S)+\omega} \Rightarrow A = -K^M \frac{1-S}{(1-S)(1-\omega)+\omega}. \tag{43}$$

Solving Eqs. (34) and (36) for this expression of A yields:

$$\bar{s} = \left(K^M \frac{(1-\omega)(1-S)}{(1-\omega)(1-S)+\omega} \right) \varepsilon,$$
$$e = \frac{(1-S)\,\boldsymbol{\varepsilon}}{(1-\omega)(1-S)+\omega} \quad \text{and}$$
$$\phi = \frac{\boldsymbol{\varepsilon}}{(1-\omega)(1-S)+\omega}. \tag{44}$$

For the Mori-Tanaka model, the strain in the inclusion not only depends on the inclusion shape and properties (through **S**) but also depends on the inclusion volume fraction. This is explained by the fact that as the volume fraction increases, the effect of inclusion interaction becomes more and more important. This model degenerates to the dilute composite model in the limit $\omega \to 0$.

Several observations can be made regarding the above solutions.

- First, as depicted in Figure 5, the value of the interaction factor A varies in terms of the volume fraction, and its variation is very different according to the model that one considers. For the mixture model, since the deformation of each phase is assumed to be the same, regardless of the volume fraction, the interaction matrix ω is constant. However, its value increases drastically with the volume fraction when the dilute model is considered, while it undergoes a relatively small increase with the Mori-Tanaka approximation. This increase is due to the fact that the contribution of the void to the overall mechanical response becomes larger as ω increases. We also note that the dilute model gives a vanishing interaction matrix at $\omega = 1 - S \approx 0.42$. These nonphysical results arise because the model is not valid when ω is greater than 0.1 and is the reason why the overall composite bulk modulus vanishes for the same value of ω.
- Second, from (39), (41), and (44), the estimation of the overall composite moduli for the three models are plotted in terms of the void volume fraction in Figure 5 and have the following expressions:

$$\bar{K} = K^M \times \begin{cases} (1-\omega) & \text{Mixture model} \\ (1-S-\omega)/(1-S) & \text{Dilute composite model} \\ (1-\omega)(1-S)/ & \\ \quad [(1-\omega)(1-S)+\omega] & \text{Mori-Tanaka model} \end{cases}. \tag{45}$$

This is consistent with the estimation of the bulk modulus given in the literature under the same assumptions. The microstructure-based model is then able to incorporate and reproduce the estimation of well-known homogenization theories.

- Third, an interesting aspect of the microstructure-based theory is that the relative contribution of matrix and voids to the overall strain are obtained by solving the governing equations. We thus gain precious information about internal deformation, which is important in physically motivated material models (to characterize plasticity at small scales or fracture initiation, for instance). To illustrate this, Figure 6 shows the relative deformation of matrix and void with respect to total deformation as predicted with the three assumptions (mixture, dilute, and Mori-Tanaka) considered here. These trends clearly show that the mixture model captures the same deformation for void and matrix while the Mori-Tanaka model describes an increase in relative void deformation with decreasing volume fraction. Finally, while the dilute model is nonphysical for a large volume fraction, it provides a fairly good representation of the relative deformation for small values of ω.
- Finally, the approach permits to naturally link micromechanical models, such as the models of Eshelby and Mura [16], to the development of the constitutive relation of materials with a microstructure. This feature is attractive for the modeling of complex material deformation, including plasticity and damage.

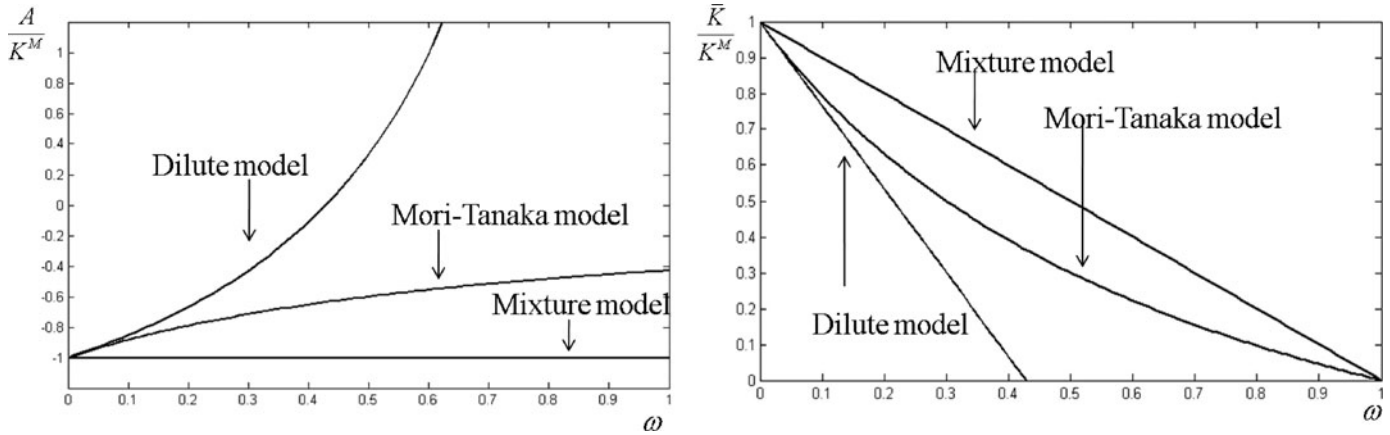

Fig. 5. Relative interaction parameter A/K^M and overall bulk modulus $\bar{K}/K^M$ in terms of void volume fraction ω using the microstructure-based theory and three different models for the interaction matrix. We used a Poisson's ratio of $\nu = 0.3$ to generate the above plots.

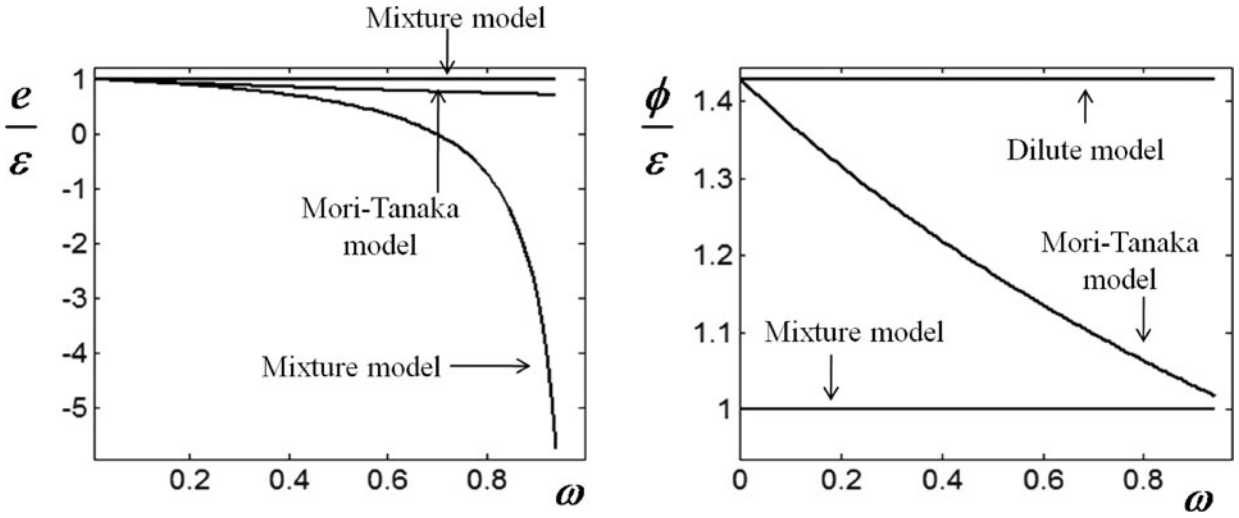

Fig. 6. Relative deformation of matrix e/ε and void ϕ/ε in terms of void volume fraction ω using the microstructure-based theory and three different models for the interaction matrix ($\nu = 0.3$).

The next example illustrates the potential of the micro-continuum theory in capturing size effect by considering the deformation profile in a fiber-reinforced composite near a stressed edge.

7. Application 2: Size Effects near a Surface of a Fiber-Reinforced Material

In this section, we consider a fiber-reinforced composite subjected to a tensile stress in the fiber direction. The choice of this example resides in the fact that the interaction of the boundary conditions and the microstructure results in the development of a "boundary layer" in which shear stresses are observed near the boundary where the stress is applied. While far from the boundary, fibers and matrix undergo the same level of deformation, due to kinematic constraints in the bulk. However, near a free boundary subjected to a stress, they deform in a different fashion due their difference in stiffness (Figure 7). This difference in tensile deformation triggers shear stresses in the matrix and at the matrix-fiber interface, which may subsequently trigger the nucleation of damage in the form of delamination. The characteristic of the "boundary layer" entirely depends on microstructure properties and arrangement. Due to the size dependence of the solution, this problem constitutes a very good benchmark to assess the capacity of the model to capture size effects.

We propose to study a simplified model of fiber-reinforced composite as follows: consider a material possessing a family of fibers oriented in the same direction, characterized by several variables: the fiber volume fraction ω, the spacing ℓ between the centerline of two adjacent matrix segments, and the uniaxial elastic moduli C^F and C^M of fibers and matrix, respectively. For simplicity, we consider a thin specimen in plane stress conditions that is deforming under the action of a distributed vertical force on its top surface, while the vertical displacement of its bottom boundary is prescribed as depicted in Figure 7.

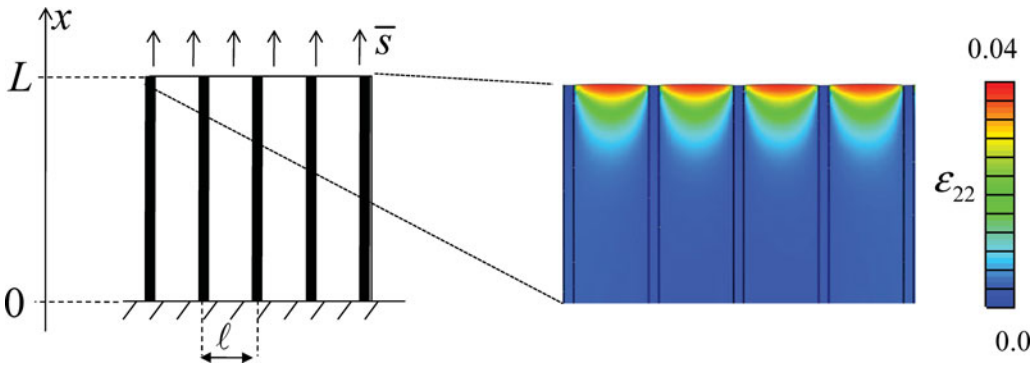

Fig. 7. Entire domain showing the structure of the fiber-reinforced composite (fibers are black) and boundary conditions. To the right are contours of tensile strains computed from a two-dimensional plane stress finite element analysis clearly displaying the boundary layer.

7.1. *Governing Equations and Boundary Conditions*

7.1.1. *Governing Equations*

For this problem, the kinematic variables consist of the uniaxial deformation of the matrix and the fibers e and ϕ, respectively. Their relation to the overall displacement u is then given by Eq. (1). For this one-dimensional problem, the governing equations (15) thus become:

$$\frac{\partial s^1}{\partial x} = 0 \quad \text{and} \quad s^1 - s^2 + \frac{\partial \tau^2}{\partial x} = 0 \quad x \in [0, L]. \tag{46}$$

7.1.2. *Boundary Conditions*

It is shown in the appendix that the above equation may be written in terms of two coupled second order linear differential equations for u and ϕ. Therefore, four boundary conditions are needed: two for u and two for ϕ. These conditions are based on the following assumptions:

- The boundary $x = 0$ is such that the displacement in both the fiber and the matrix vanishes.
- The length L is large enough such that all boundary effects vanish at this end. In other words, the strains at $x = 0$ are those of the bulk composite, that is $\varepsilon(0) = \phi(0) = e(0)$ and these strains are constant, $d\phi/dx(0) = 0$.
- The composite is subject to an average tensile stress $\bar{\sigma}$ acing in the fiber direction. This may be written in $x = 0$ as follows: $(1-\omega)K^M e(0) + \omega K^F \phi(0) = \bar{\sigma}$. Using the assumption from the previous entry, this is written as: $\bar{K} du/dx(0) = \bar{\sigma}$, where $\bar{K} = (1-\omega)K^M + \omega K^F$ is the overall modulus of the composite.

In a more compact form, the boundary conditions for this problem are thus written as follows:

$$\begin{cases} u(0) = 0 \\ \dfrac{du}{dx}(0) = \dfrac{\bar{\sigma}}{\bar{K}} \end{cases} \quad \begin{cases} \phi(0) = e(0) \\ \dfrac{d\phi}{dx}(0) = 0 \end{cases}. \tag{47}$$

7.2. *Derivation of the Elastic Matrix*

Assuming small deformation and an elastic response of the constituents, the linear stress-strain relation (13) may be used in the following form:

$$\begin{pmatrix} s^1 \\ s^2 \\ \tau^2 \end{pmatrix} = \begin{bmatrix} C^M & \omega A & 0 \\ -(1-\omega)A & C^F & 0 \\ 0 & 0 & G \end{bmatrix} \cdot \begin{pmatrix} e \\ \phi \\ \partial\phi/\partial x \end{pmatrix}. \tag{48}$$

The first two diagonal terms are the stiffness of the matrix and fiber, respectively, A is the interaction constant (arising from the fiber/matrix interaction) and G governs the magnitude of the stress couple during inhomogeneous deformation. The constant A is determined by observing that, during homogeneous deformation, the fiber and the matrix undergo identical tensile strains: $e = \phi$. Referring to the analysis of the previous section, this is equivalent to taking $M = 1$ in Eq. (16). Referring to (17), this leads to:

$$A = C^F - C^M. \tag{49}$$

The determination of the constant G arises from a micromechanical model of fiber's inhomogeneous deformation. The analysis relies on two points:

- The energy equivalence between the energy stored by shear strains in the matrix and that stored by the gradient of the matrix strain ϕ;
- The fiber equilibrium during inhomogeneous deformation.

During inhomogeneous deformation, the difference in tensile strain between matrix and fiber trigger the development of shear strains in the matrix [18, 19]. This strain acts against the development of further inhomogeneous strain, and is responsible for restoring homogeneous deformation at a finite distance from the homogeneities. Matrix shear strains are thus responsible for size effects in the material and are innovatively accounted for in our model, by the couple stress r. Based on these observations, we state that the strain energy stored in the matrix is equal to the energy associated with the fiber strain gradient:

$$\omega r \frac{\partial \phi}{\partial x} = (1-\omega)\tau^M \gamma^M, \tag{50}$$

where the left-hand side is the energy associated with the couple stress according to (3) and τ^M and γ^M are the shear stress and strain in the matrix, respectively. Denoting G^M as the shear modulus of the matrix, (29) can be rewritten as:

$$\frac{\omega}{1-\omega} G \frac{\partial \phi}{\partial x}\frac{\partial \phi}{\partial x} = \frac{\tau^M \tau^M}{G^M}, \tag{51}$$

where we used the linear elastic relations $r = G\partial\phi/\partial x$ and $\tau = G^M \gamma^M$. Let us now consider the equilibrium of a fiber segment during inhomogeneous deformation as depicted in Figure 8. The deformation of the segment arises from the action of tensile stresses on each side of the fiber and the

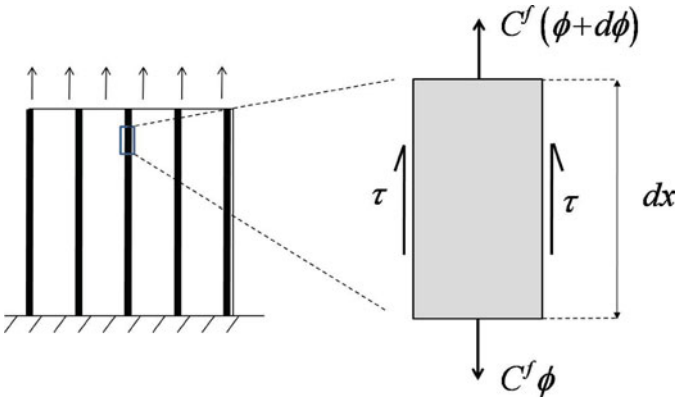

Fig. 8. Equilibrium of a fiber segment.

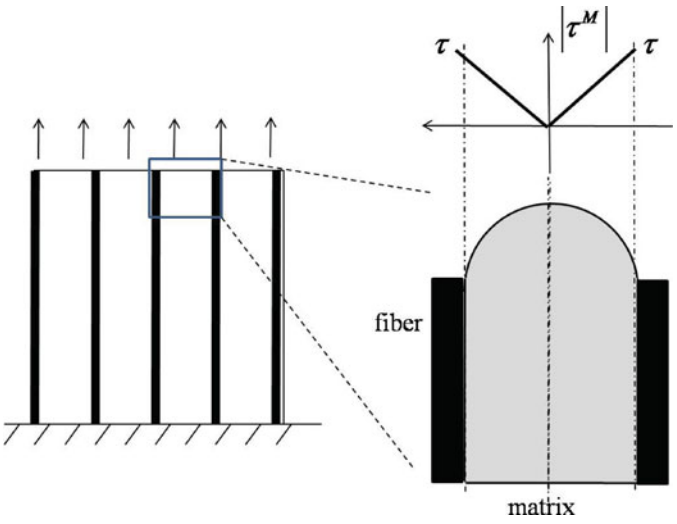

Fig. 9. Distribution of shear strain in the matrix.

action of a shear stress τ transmitted by the matrix across the fiber/matrix interface.

Referring to Figure 8, writing the equilibrium of the fiber segment gives a relationship between the interface shear stress τ and the variation of fiber strain ϕ as follows:

$$\tau = \frac{\ell \omega C^F}{2} \frac{d\phi}{dx}. \tag{52}$$

It is possible to determine the average amount of shear strain in the matrix $|\tau^M|$ as a function of the interfacial shear stress τ by assessing at the strain profile in a matrix segment. In this study, we introduce a coefficient α depending on the shear strain profile, such that $|\tau^M| = \alpha\tau$. Using this expression, together with (30) and (31), the unknown coefficient G can be written as:

$$G = \omega(1-\omega)\frac{\ell^2 \alpha^2 C^F C^F}{4G^M}. \tag{53}$$

Note that G contains information about the intrinsic length scale of the material; this term, therefore, plays an important role in capturing size effects near a stressed boundary. The linear elastic constitutive relation (13) can finally be written in

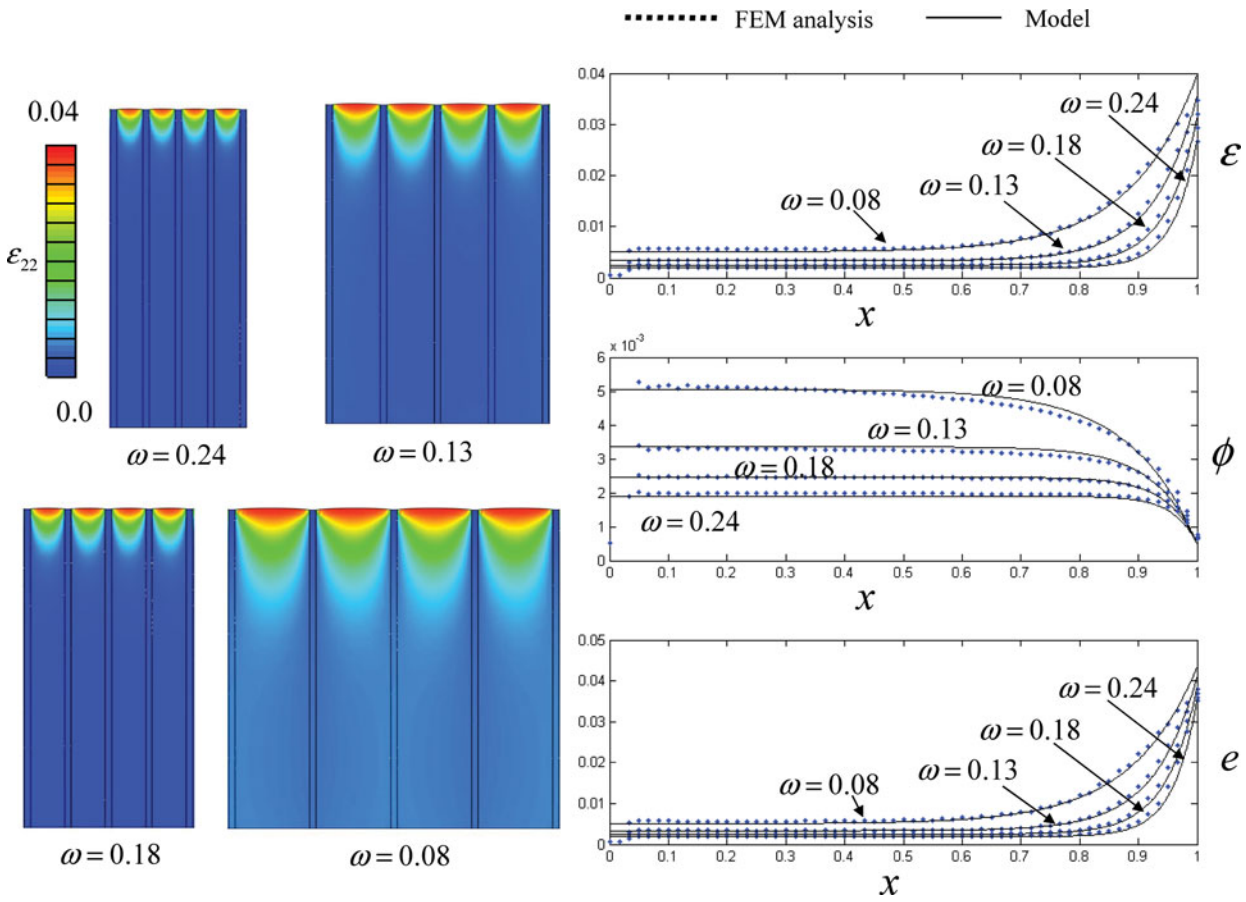

Fig. 10. Finite element computation of a fiber-reinforced composite subject to distributed load on its boundary. Comparison of strain near a stressed edge for different fiber volume fraction calculated from the model and finite element computations: (a) ω = 0.08, (b) ω = 0.13, (c) ω = 0.18, (d) ω = 0.24.

the following form:

$$\begin{pmatrix} s^1 \\ s^2 \\ \tau^2 \end{pmatrix} = \begin{bmatrix} C^M & \omega(C^F - C^M) & 0 \\ -(1-\omega)(C^F - C^M) & C^F & 0 \\ 0 & 0 & f(1-\omega)\dfrac{\ell^2\alpha^2 C^F C^F}{4G^M} \end{bmatrix} \cdot \begin{pmatrix} e \\ \phi \\ \partial\phi/\partial x \end{pmatrix}. \tag{54}$$

In the present work, we assume that the shear strain distribution is linear as depicted in Figure 9, ranging from zero in the middle of a matrix segment to its maximum value at the matrix/fiber interface. This implies that the average shear strain is half its maximum value, and hence, $\alpha = \frac{1}{2}$.

7.3. *Solution and Comparison with Two-Dimensional Finite-Element Analysis*

Referring to the appendix, the analytical solution of the governing equations and boundary conditions given by (25) and (26), together with the constitutive relation (33), is given by:

$$\begin{cases} \phi(x) = \bar{\sigma}\left\{\left(\dfrac{c}{ad-bc} + \dfrac{1}{C^F}\right)\dfrac{e^{Ax} + e^{-Ax}}{e^{AL} + e^{-AL}} - \dfrac{c}{ad-bc}\right\} \\ u(x) = \bar{\sigma}\left\{\dfrac{d}{ad-bc}x - \dfrac{1}{aA}\left(\dfrac{bc}{ad-bc} + \dfrac{b}{C^F}\right) \times \dfrac{e^{Ax} - e^{-Ax}}{e^{AL} + e^{-AL}}\right\} \end{cases}, \tag{55}$$

where $A = \sqrt{\frac{1}{g}\left(\frac{bc}{a} - d\right)}$. In the above equations, the coefficients are $a = \frac{C^M}{1-\omega}$,

$$b = \frac{\omega}{(1-\omega)}[(1-\omega)C^F - (2-\omega)C^M],$$

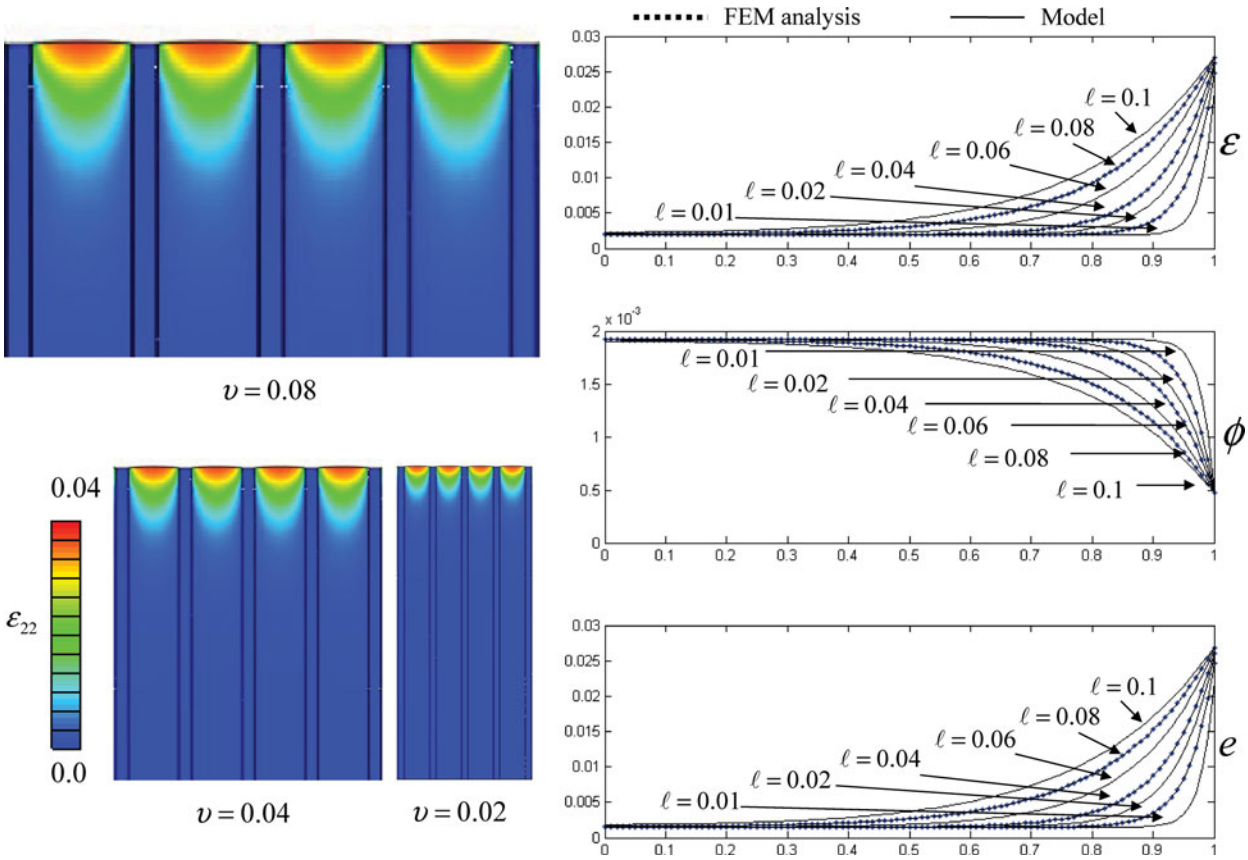

Fig. 11. Finite element computation of a fiber-reinforced composite subject to distributed load on its boundary for a fixed volume fraction and various fiber diameters υ. Comparison of strain near a stressed edge for different fiber diameters calculated from the model and finite element computations.

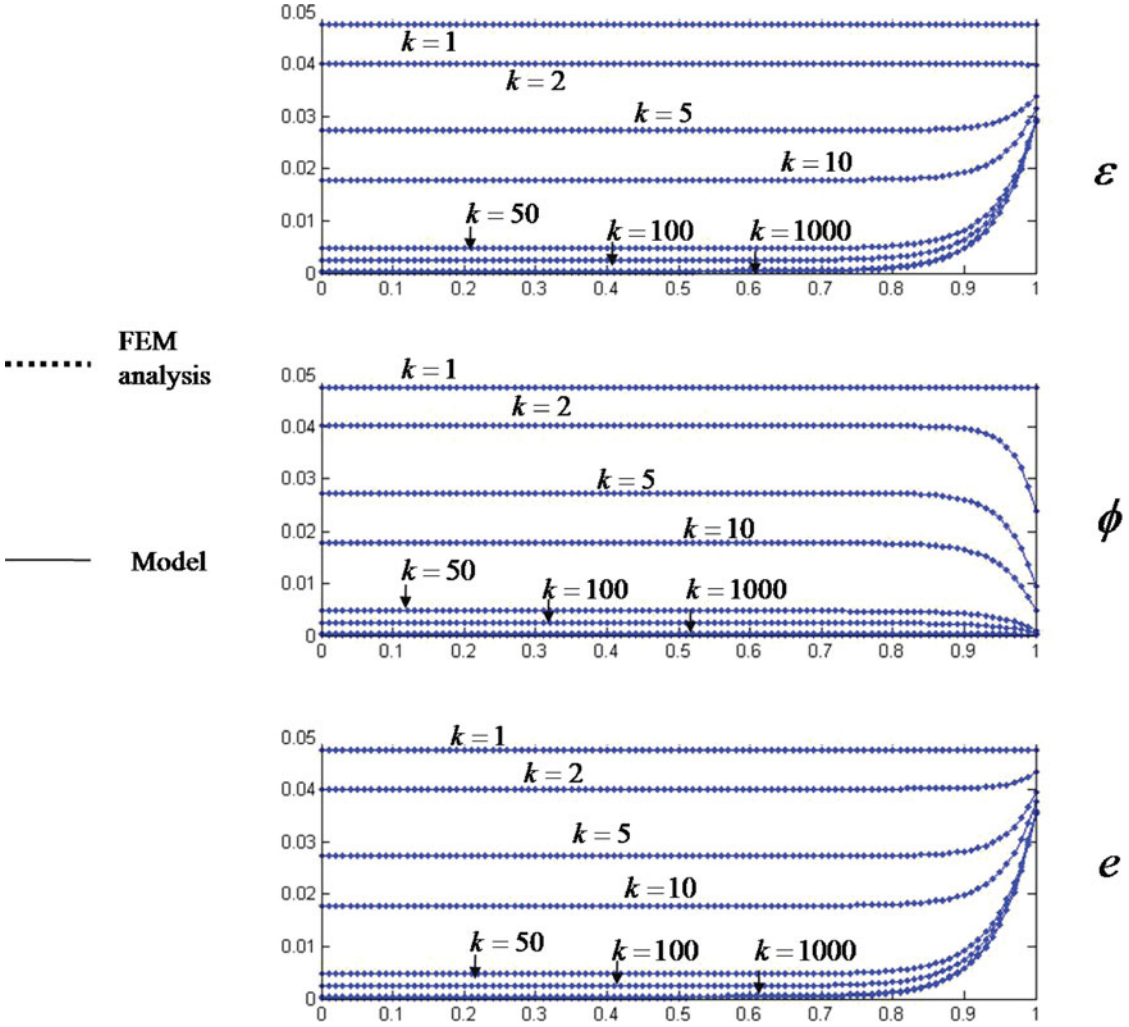

Fig. 12. Comparison of strain near a free edge for different fiber/matrix stiffness ratio $k = C^F/C^M$.

$$c = \frac{1}{(1-\omega)}[\omega C^M + (1-\omega)C^F],$$
$$d = -\left[C^F + \frac{\omega}{1-\omega}C^M\right],$$

and $g = G$. We now propose to assess the model by studying how changes in microstructural properties affect local and global deformation in the material. To assess the accuracy of our solution in each case, we also compare it with two-dimension plain strain finite element computations of a fiber-reinforced composite subjected to the same boundary conditions. We first assess the variation of boundary layer with fiber volume fraction, for fixed fiber radius and fixed fiber/matrix stiffness ratio. Figure 10 shows the profile of average strain ε, heterogeneous defect strain ϕ, and average matrix strain e calculated by the analytical model whose solution is given in (34) and compared with the plane stress finite element analysis.

The analytical model accurately captures the variation of strain profile near a stressed boundary for ε, ϕ, and e. We notice that the characteristic length scale decreases with increasing fiber volume fraction. Since fibers are much stiffer than the matrix, the fiber deformation is much smaller than that of the matrix, and hence, ϕ decreases near the boundary. As the distance to the stressed surface increases, we notice two points: (a) the deformations e and ϕ converge to the homogeneous deformation ε since the deformation of the matrix and fibers are the same in the bulk material and (b) the average strain ε converges to the strain that is calculated with conventional homogenization theory.

Next, we assess the solution of the analytical model for changing fiber diameter at fixed volume fraction ($\omega = 0.24$). Figure 11 displays the tensile strain profile given by finite element simulation for three fiber diameters: $\upsilon = 0.08$, $\upsilon = 0.04$, and $\upsilon = 0.02$ and gives the comparison between finite element simulation and model for various fiber diameters (note that the comparison is provided for $\ell = 0.02$, $\ell = 0.04$, and$\ell = 0.08$). We observe a very good agreement between the plane stress analysis and the solution provided by the micro-continuum model. As expected, the size of the boundary layer increases with increasing fiber diameter. We also note that the strain on the boundary is independent of the fiber diameter.

Finally, we explore the effect of changing the ratio $k = C_f/C_m$ of fiber and matrix stiffness as depicted in Figure 12. We find an excellent agreement between the finite element method (FEM) simulation and the model for values of the parameter k ranging from 1 (for homogeneous material) to 1000 (in the case of stiff fibers). We observe that the solution for e and ϕ converges to the homogeneous solution (no boundary layer) as k tends to 1. We also observe that the variation of strain in the matrix near the boundary increases significantly as the fiber stiffness increases.

8. Conclusion

This article presented a novel micro-continuum theory where the strain decomposition is based on phases separation rather than length scales separation [12]. This results in a meaningful physical definition of kinematic variables and associated stresses. This feature is important for the development of theoretical and computational models that relate microstructural features to material response. Similarly to micromorphic theory, the new theory is able to describe size effects when the gradient of heterogeneous defect deformation becomes significant (such as in fracture, localization, and boundary layers). Moreover, it can describe the heterogeneous deformation of microstructural elements (voids, particles, fibers) when the deformation is macroscopically homogeneous.

Two applications are presented to highlight the strength of the model, and solutions are presented in the one-dimensional case. First, the volumetric deformation of an elastic material with defect was considered. The constitutive relation reconciles micromechanics in the sense of Mura and Eshelby to the present formulation. In this context, our results show that the model permits to characterize the macroscopic strain, but also the heterogeneous deformation of defects within the material. Furthermore, we showed that the elastic modulus is different than that predicted by conventional homogenization procedures in that it accounts for the difference of deformation between defect and matrix. A better prediction for the average modulus is therefore expected; this will be studied in detail in further studies. Second, the example of size effects near the stressed surface of a fiber-reinforced composite is accurately captured by the model. A simple elastic constitutive relation is derived based on micromechanical arguments. The comparison of the model with two-dimensional finite element simulation shows that the model works very well in capturing the material behavior, size effects, and the trends in the response with respect to change of material parameters. In short, the presented micro-continuum model possesses the following contributions:

- It is inexpensive, accurate, and allows to relate microstructural features to the mechanical response of material, including size dependency.
- It describes the internal evolution of the microstructure during deformation thanks to the incorporation of additional kinematic fields.
- The determination of the constitutive relation relies on simple micromechanics models.

While applications used to illustrate the model are based on very simple material behaviors (linear elasticity, one-dimensional problems), the micro-continuum theory may be a good candidate for a new generation of computational damage model that can represent size effects and are physically based. For instance, the development of such models is extremely important for material design.

Funding

FJV gratefully acknowledges funding from NSF grant number CMMI-0900607 in support of this research.

References

[1] S. Nemat-Nasser and M. Hori, Micromechanics: Overall Properties of Heterogeneous Materials, North-Holland, Amsterdam, 1999.
[2] Z. Bazant, Why continuum damage is nonlocal: Micromechanical arguments, J. Eng. Mech., vol. 117, pp. 1070–1087, 1991.
[3] Z. Bazant and D. Novak, Nonlocal integral formulations of plasticity and damage: Survey of progress, J. Eng. Mech., vol. 128, pp. 1119–1149, 2002.
[4] N.A. Fleck and J.W. Hutchinson, Strain gradient plasticity, Adv. Appl. Mech., vol. 33, pp. 295–361, 1997.
[5] N.A. Fleck and J.W. Hutchinson, A reformulation of strain gradient plasticity, J. Mech. Phys. Solids, vol. 49, pp. 2245–2271, 2001.
[6] N.A. Fleck, G.M. Muller, M.F. Ashby, and J.W. Hutchinson, Strain gradient plasticity: Theory and experiment, Acta Metall. Mater., vol. 42, pp. 475–487, 1994.
[7] E. Cosserat and F. Cosserat, Theorie des Corps Deformables, A Hermann et Fils, Paris, France, 1909.
[8] A.C. Eringen, Microcontinuum Field Theories 1: Foundations and Solids, Springer-Verlag, New York, 1999.
[9] P. Germain, The method of virtual power in continuum mechanics. Part 2: Microstrucure, SIAM J. Appl. Math., vol. 25, pp. 556–575, 1973.
[10] H.B. Muhlaus and I. Vardoulakis, The thickness of shear band in granular materials, Geotechnique, vol. 237, pp. 271–283, 1987.
[11] R. Deborst, A generalization of j2-flow theory for polar continua, Comput. Meth. Appl. Mech. Eng., vol. 103, pp. 347–362, 1993.
[12] F.J. Vernerey, W.K. Liu, and B. Moran, Multi-scale micromorphic theory for hierarchical materials, J. Mech. Phys. Solids, vol. 55, pp. 2603–2651, 2007.
[13] F.J. Vernerey, W.K. Liu, B. Moran, G. Olson, A micromorphic model for the multiple scale failure of heterogeneous materials, J. Mech. Phys. Solids, vol. 56, no. 4, pp. 1320–1347, 2008.
[14] M. Jirasek, Nonlocal models for damage and fracture: comparison of approaches, Int. J. Solids Struc., vol. 35, no. 32, pp. 4133–4145, 1998.
[15] O.B. Pedersen, Thermoelasticity and plasticity of composites. I. Mean field theory, Acta Metall., vol. 31, pp. 1795–1808, 1983.
[16] T. Mura, Micromechanics of Defects in Solids, Kluwer Academic Publishers, Dordrecht, 1987.
[17] Y. Benveniste, A new approach to the application of Mori-Tanaka's theory in composite materials, Mech. Mater., vol. 6, pp. 147–157, 1987.
[18] J.C. Iatridis, Mechanisms for mechanical damage in the intervertebral disc annulus fibrosus, J. Biomechanics, vol. 37, pp. 1165–1175, 2004.

[19] S. Swanson, Introduction to Design and Analysis with Advanced Composite Materials, Prentice-Hall, Upper Saddle River, NJ, 1997.

Appendix

Solution for the Inhomogeneous Surface Deformation under Traction Boundary Conditions

For the one-dimensional example studied in this article, the governing equations are written in (46), subject to boundary conditions (47) and linear elastic constitutive relation (54). The equation can be rewritten in terms of the primary variables u and ϕ, leading to the following system of differential equations:

$$\begin{cases} a\dfrac{d^2u}{dx^2} + b\dfrac{d\phi}{dx} = 0 \\ c\dfrac{du}{dx} + d\phi + g\dfrac{d^2\phi}{dx^2} = 0 \end{cases} \qquad x \in [0, l], \tag{A1}$$

With boundary conditions:

$$\begin{cases} u(0) = 0 \\ \dfrac{du}{dx}(0) = \dfrac{\bar{\sigma}}{\bar{K}} \end{cases} \quad \begin{cases} \dfrac{du}{dx}(0) = \phi(0) \\ \dfrac{d\phi}{dx}(0) = 0 \end{cases}. \tag{A2}$$

In the above equations, the coefficients are $a = \frac{C^M}{1-\omega}$, $b = \frac{\omega}{(1-\omega)}[(1-\omega)C^F - (2-\omega)C^M]$, $c = \frac{1}{(1-\omega)}[\omega C^M + (1-\omega)C^F]$, $d = -[C^F + \frac{\omega}{1-\omega}C^M]$, and $g = G$. This system of equations can be reduced to single ordinary differential equations by integrating the first equation once to obtain:

$$\begin{cases} \dfrac{du}{dx} = -\dfrac{b}{a}\phi + K \end{cases} \quad x \in [0, L], \tag{A3}$$

where K can be determined using the boundary condition $du/dx(0) = \phi(0) = \bar{\sigma}/\bar{K}$:

$$K = \frac{\bar{\sigma}}{a}. \tag{A4}$$

Using this equality in the second equation leads to the following differential equation for ϕ:

$$g\frac{d^2\phi}{dx^2} + \left(d - \frac{bc}{a}\right)\phi + cK = 0. \tag{A5}$$

Solving this equation and using the boundary condition $d\phi/dx(0) = 0$ leads to the following expression for ϕ:

$$\phi(x) = \left(\frac{acK}{ad-bc} + \frac{\bar{s}}{C^F}\right)\frac{e^{Ax} + e^{-Ax}}{e^{AL} + e^{-AL}} - \left(\frac{ac}{ad-bc}\right)K, \tag{A6}$$

where $A = \sqrt{\frac{1}{g}(\frac{bc}{a} - d)}$. These coefficients are function of boundary conditions and express the evolution of ϕ with loading. Knowing the expression for ϕ, one can now solve the first differential equation in (A1), which is rewritten as:

$$\frac{du}{dx} = \left(-\frac{bcK}{ad-bc} - \frac{b}{a}\frac{\bar{s}}{C^F}\right)\frac{e^{Ax} + e^{-Ax}}{e^{AL} + e^{-AL}} + \left(\frac{bc}{ad-bc} + 1\right)K, \tag{A7}$$

with boundary conditions:

$$u(0) = 0. \tag{A8}$$

This leads to an expression for the displacement $u(x)$ as follows:

$$u(x) = \frac{d\bar{\sigma}}{ad-bc}x + \frac{1}{aA}\left(-\frac{bc\bar{\sigma}}{ad-bc} - b\frac{\bar{\sigma}}{C^F}\right) \times \frac{e^{Ax} - e^{-Ax}}{e^{AL} + e^{-AL}}. \tag{A9}$$

The expression for ϕ can also be rewritten in terms of the surface stress $\bar{s}$:

$$\phi(x) = \left(\frac{c\bar{\sigma}}{ad-bc} + \frac{\bar{\sigma}}{C^F}\right)\frac{e^{Ax} + e^{-Ax}}{e^{AL} + e^{-AL}} - \frac{c\bar{\sigma}}{ad-bc}. \tag{A10}$$